Resource Allocation for URLLC-Oriented Two-Way UAV Relaying

***Abstract*—Due to the high altitude and deployment flexibility, unmanned aerial vehicles (UAVs) can be used as relays to avoid obstacles and extend the coverage of wireless networks. On the other hand, ultra-reliable and low-latency communication (URLLC) is often required to deliver the information reliably and timely for many emerging applications. In this correspondence, we combine the advantages of both UAV and URLLC to investigate the resource allocation for a URLLC-enabled two-way UAV relaying system. Our goal is to maximize the transmission rate of the backward link with the constraint of URLLC requirement for the forward link. The optimization is non-convex and difficult to solve. Therefore, the optimization variables are divided to several blocks, and three sub-problems are formulated and solved. Finally, an iterative algorithm is proposed to solve these sub-problems alternately. Simulation results show that the proposed joint optimization scheme can achieve excellent performance for the URLLC-enabled two-way UAV relaying system.**

***Index Terms*—Resource allocation, two-way relay, UAV, URLLC.**

I. INTRODUCTION

Unmanned aerial vehicle (UAV)-assisted communication has received widespread attention because of its flexibility and excellent channel condition [1]. Specifically, UAVs can fly flexibly to avoid obstacles and achieve better air-to-ground channels than the terrestrial ones. In emergency scenarios, such as disaster rescue, the terrestrial infrastructure may not be available for providing reliable wireless service. Fortunately, UAVs can be deployed under complex environment and avoid obstacles to provide wireless coverage due to the mobility [2].

In future UAV networks, full coverage, strong reliability, low latency and high security are needed to satisfy the requirements of various applications [3], [4]. Ultra-reliable and low-latency communication (URLLC) is one of the three main applications of the fifth generation (5G) network. In some mission-critical applications, the packet delay should be no more than 1 ms, and the decoding error should be less than 10^{-5} [5]. Since UAVs are wirelessly controlled, URLLC is also one of the essential requirements of air-to-ground communications to ensure safe flight. This was investigated in [6] and [7], where the communication performance was enhanced by optimizing the blocklength. In addition, in many critical applications, remote devices are required to transmit essential information through UAVs with constraints on latency and reliability. For instance, in a safety alarm system, ground devices need to send alarms to UAVs under the URLLC requirement [8]. For an energy-limited ground device, its uplink transmit power was minimized under the constraints of URLLC by Chan *et al.* via jointly optimizing the device scheduling, power allocation and UAV deployment [9]. For UAVs equipped with directional antennas, optimizing the beamwidth is also beneficial for the URLLC performance [10]. In addition to remote control of UAV and devices, data transmission is another key requirement for various UAV applications, such as monitoring and data collecting. Thus, jointly considering the URLLC and data transmission is a promising direction. In [11], the network slicing problem was investigated by Yang *et al.* to provide efficient broadband communication while satisfying the URLLC requirement. Similar scenario was also investigated by Yang *et al.* in [12], where power control was employed to enhance the URLLC performance under the broadband transmission requirements.

–

One of the most important applications of UAV communication is relaying [13]. As is known, relaying is an effective way to achieve ubiquitous wireless coverage in harsh environments [14], [15]. Thus, the URLLC of UAV relaying networks has been investigated in literature. In UAV-enabled relaying networks, the ground station can control the remote devices through the UAV relay. Due to the latency requirement, a URLLC relaying link should be established. With the given latency requirement, optimizing the UAV location and blocklength is an effective way to reduce the block error probability [16], [17]. This work was then extended to multiple UAV relays in [18]. In [19], the URLLC control of multiple UAVs and the broadband UAV-enabled relaying were jointly optimized by Xi *et al.*.

In this correspondence, we combine URLLC with data transmission, and propose a two-way UAV-enabled relaying scheme. Due to the obstacle between the base station (BS) and the remote device, a UAV is deployed as a two-way relay to connect them. We maximize the backward transmission rate via resource allocation under the URLLC of the forward link.

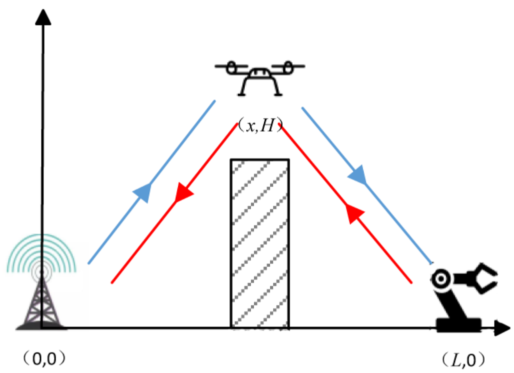

Fig. 1: URLLC-enabled two-way UAV relaying system.

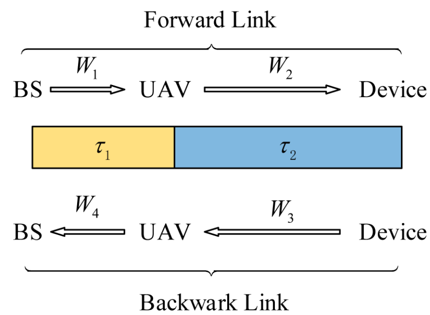

Fig. 2: Transmission diagram of forward and backward links.

To tackle this optimization, we first solve three sub-problems alternately and then propose an efficient iterative algorithm to obtain the approximate solution. Simulation results show the effectiveness of the proposed scheme.

II. System Model

As shown in Fig. 1, a remote device is performing the delay-sensitive mission under the control of a BS. At the same time, the data collected by the device are uploaded to the BS. The direct link between the device and the BS is blocked. Therefore, a UAV is deployed for two-way relaying between the BS and device. We denote the BS-UAV-device link as the forward link, where the control command is transmitted. In the forward link, the latency and decoding error probability are strictly constrained to maneuver the device timely and reliably. Similarly, the device-UAV-BS link is denoted as the backward link, where a large amount of data collected by the device are sent to the BS efficiently. The aim of the two-way relaying system is to increase the transmission rate of backward link when the URLLC is satisfied in the forward link.

As shown in Fig. 1, similar to [17], we assume that the BS, the UAV and the device are on a two-dimensional plane, and the UAV is hovering at a fixed height H. The locations of the BS and the device are $(0,0)$ and $(L,0)$ respectively, and the location of the UAV is (x,H), where $0 \leq x \leq L$. The distance from the BS to the UAV and that from the UAV to the device can be calculated as

$$d_1 = \sqrt{x^2 + H^2}, \tag{1}$$

$$d_2 = \sqrt{(L-x)^2 + H^2}. \tag{2}$$

The channel power gain from the BS to the UAV, and that from the UAV to the device are denoted as h_1 and h_2, respectively. When the UAV is flying high enough, the line-of-sight (LoS) is achieved in the air-to-ground channel. Thus, h_1 and h_2 can be represented as

$$h_1 = \frac{\beta_0}{H^2 + x^2}, \tag{3}$$

$$h_2 = \frac{\beta_0}{(L-x)^2 + H^2}, \tag{4}$$

where β_0 is channel power gain at the reference of $d_0 = 1$.

III. URLLC-Enabled Two-Way UAV Relaying

We introduce the transmission process of the forward and backward links, and then present the optimization problem.

A. Forward Link

In the forward link, URLLC is required to control the device effectively. The maximum delay of the forward link is τ. Considering the decode-and-forward (DF) relaying, the transmission duration for the BS-UAV link and the UAV-device link can be denoted as τ_1 and τ_2, respectively. We have $\tau_1 + \tau_2 \leq \tau$. The bandwidth and decoding error probability of the BS-UAV link are W_1 and ϵ_1, respectively. Likewise, the bandwidth and decoding error probability of the UAV-device link are W_2 and ϵ_2, respectively.

In the forward link, the received signal-to-noise ratio (SNR) at the UAV and the device can be expressed as

$$\gamma_1 = \frac{P_a h_1}{W_1 N_0}, \tag{5}$$

$$\gamma_2 = \frac{P_u h_2}{W_2 N_0}, \tag{6}$$

where N_0 is the noise power spectral density, P_a is the transmit power of BS, and P_u is the transmit power of UAV.

To perform the remote control successfully, at least C_0 bits of data need to be transmitted under the URLLC requirement. According to [7] and [20], the constraints can be expressed as

$$\tau_1 W_1 \left(\log_2(1+\gamma_1) - \sqrt{\frac{V_1}{W_1 \tau_1}} \log_2(e) Q^{-1}(\epsilon_1) \right) \geq C_0, \tag{7}$$

$$\tau_2 W_2 \left(\log_2(1+\gamma_2) - \sqrt{\frac{V_2}{W_2 \tau_2}} \log_2(e) Q^{-1}(\epsilon_2) \right) \geq C_0, \tag{8}$$

where

$$V_1 = 1 - 1/\left(1 + \gamma_1^2\right), \tag{9}$$

$$V_2 = 1 - 1/\left(1 + \gamma_2^2\right), \tag{10}$$

are the channel dispersions.

Since the DF relaying is carried out at the UAV, the total decoding error probability can be denoted as

$$\epsilon = 1 - (1-\epsilon_1)(1-\epsilon_2) = \epsilon_1 + \epsilon_2 - \epsilon_1 \epsilon_2. \tag{11}$$

To achieve high reliability, ϵ_1 and ϵ_2 are usually very small. Therefore, the total decoding error probability can be approximated as

$$\epsilon \approx \epsilon_1 + \epsilon_2. \tag{12}$$

From (7) and (8), we can see that ϵ_1 and ϵ_2 are in the inverse of the Q function, which are difficult to optimize. For ease of analysis, assume that the decoding error probabilities ϵ_1 and ϵ_2 are fixed. Then, we have $\epsilon \leq \epsilon_1+\epsilon_2$, i.e., the total decoding error probability is no more than $\epsilon_1+\epsilon_2$.

B. Backward Link

In the backward link, the device needs to send its collected data back to the BS. As shown in Fig. 2, the transmission duration for the device-UAV link and the UAV-BS link can be denoted as τ_2 and τ_1, respectively. Similar to the forward link, the UAV works in the DF mode. The received SNR at the UAV and the BS can be denoted as

$$\gamma_3 = \frac{P_b h_2}{W_3 N_0}, \tag{13}$$

$$\gamma_4 = \frac{P_u h_1}{W_4 N_0}, \tag{14}$$

where P_b is the transmit power of the device, and W_3 and W_4 are the bandwidth of the device-UAV link and the UAV-BS link, respectively. Note that the forward link and the backward link work in the frequency-division mode, with a total bandwidth W. Thus, we have $W_1+W_4 \leq W$ and $W_2+W_3 \leq W$ for the durations τ_1 and τ_2, respectively.

Since the backward link is delay-tolerant, its average transmission rate can be expressed as

$$R_0 = \min\left\{\frac{\tau_2 W_3 \log_2(1+\gamma_3)}{\tau}, \frac{\tau_1 W_4 \log_2(1+\gamma_4)}{\tau}\right\}. \tag{15}$$

C. Problem Formulation

In this paper, we aim at maximizing the average transmission rate of the backward link under the URLLC constraint of the forward link, with respect to the transmission duration, the bandwidth and the UAV location. For ease of analysis, we introduce the slack variable η, and the optimization problem can be formulated as

$$\begin{aligned}
&\max_{\eta,\boldsymbol{\tau},\mathbf{W},x} \ \eta && (16a)\\
&\ s.t. \ \tau_2 W_3 (\log_2(1+\gamma_3)) \geq \eta, && (16b)\\
&\qquad \tau_1 W_4 (\log_2(1+\gamma_4)) \geq \eta, && (16c)\\
&\qquad W_1+W_4 \leq W, && (16d)\\
&\qquad W_2+W_3 \leq W, && (16e)\\
&\qquad \tau_1+\tau_2 \leq \tau, && (16f)\\
&\qquad (7) \text{ and } (8), && (16g)
\end{aligned}$$

where $\boldsymbol{\tau} \triangleq \{\tau_1,\tau_2\}$ and $\mathbf{W} \triangleq \{W_1,W_2,W_3,W_4\}$. (16d) and (16e) are the bandwidth constraints. (16f) is the duration constraint. (16g) are the URLLC constraints of the forward link. The problem (16) is difficult to solve due to the non-convex constraints. Thus, in the following section, it is divided into several sub-problems and solved separately.

IV. Problem Transformation and Solution

In this section, (16) is divided into three sub-problems, i.e., the duration allocation problem, the bandwidth allocation problem and the location optimization problem. Then, the three sub-problems are transformed into tractable forms and solved approximately. Finally, an iterative algorithm is proposed to solve the original problem (16) alternately.

A. Transmission Duration Allocation

With fixed bandwidth and location, the optimization problem (16) can be transformed as

$$\begin{aligned}
&\max_{\eta,\boldsymbol{\tau}} \ \eta && (17a)\\
&\ s.t. \ (7),\ (8),\ (16b),\ (16c) \text{ and } (16f). && (17b)
\end{aligned}$$

In the problem (17), only the constraints (7) and (8) are not convex. Define the left hand side of (7) and (8) as $f_1(\tau_1)$ and $f_2(\tau_2)$, respectively. It can be easily verified that they are convex with respect to τ_1 and τ_2. Thus, their lower bounds $f_1^{LB}(\tau_1)$ and $f_2^{LB}(\tau_2)$ at given points τ_{10} and τ_{20} can be obtained by their first-order Taylor series as

$$f_1(\tau_1) \geq f_1(\tau_{10}) + f_1'(\tau_{10})(\tau_1-\tau_{10}) = f_1^{LB}(\tau_1), \tag{18}$$

$$f_2(\tau_2) \geq f_2(\tau_{20}) + f_2'(\tau_{20})(\tau_2-\tau_{20}) = f_2^{LB}(\tau_2), \tag{19}$$

where

$$f'(\tau_{10}) = W_1 \log_2(1+\gamma_1) - \frac{1}{2}\sqrt{\frac{V_1}{\tau_{10} W_1}} \log_2(e) Q^{-1}(\epsilon_1), \tag{20}$$

$$f'(\tau_{20}) = W_2 \log_2(1+\gamma_2) - \frac{1}{2}\sqrt{\frac{V_2}{\tau_{20} W_2}} \log_2(e) Q^{-1}(\epsilon_2). \tag{21}$$

With any feasible points τ_{10} and τ_{20}, the solution to the following optimization problem is a feasible solution to (17), i.e., (17) can be approximately solved via the following convex problem as

$$\begin{aligned}
&\max_{\eta,\boldsymbol{\tau}} \ \eta && (22a)\\
&\ s.t. \ f_1^{LB}(\tau_1) \geq C_0, && (22b)\\
&\qquad f_2^{LB}(\tau_2) \geq C_0, && (22c)\\
&\qquad (16b),\ (16c) \text{ and } (16f). && (22d)
\end{aligned}$$

(22) is convex and can be solved by using optimization toolboxes such as CVX.

It is worth noting that the solution to the problem (22) is a feasible solution to the problem (17), and the solution to (17) is a feasible solution to the original problem (16). Thus, the proposed approximation can obtain a sub-optimal solution for the original problem.

B. Bandwidth Allocation

With the duration and location fixed, the optimization problem (16) can be rewritten as

$$\max_{\eta,\mathbf{W}} \ \eta \tag{23a}$$
$$s.t. \ (7), \ (8), \ (16\text{b}), \ (16\text{c}), \ (16\text{d}) \text{ and } (16\text{e}). \tag{23b}$$

It can be easily verified that in the problem (23), only (7) and (8) are not convex with respect to $\mathbf{W}$. Following the analysis in [10], V_1 and V_2 can be approximated as 1 when the SNR exceeds 5 dB, which is almost true in URLLC constrained systems. Therefore, we assume $V_1 = V_2 = 1$. After approximation, the problem (23) can be rewritten as

$$\max_{\eta,\mathbf{W}} \ \eta \tag{24a}$$
$$s.t. \ \tau_1 W_1\left(\log_2(1+\gamma_1) - \sqrt{\frac{1}{W_1\tau_1}}\log_2(e)Q^{-1}(\epsilon_1)\right) \geq C_0, \tag{24b}$$
$$\tau_2 W_2\left(\log_2(1+\gamma_2) - \sqrt{\frac{1}{W_2\tau_2}}\log_2(e)Q^{-1}(\epsilon_2)\right) \geq C_0, \tag{24c}$$
$$(16\text{b}), \ (16\text{c}), \ (16\text{d}) \text{ and } (16\text{e}). \tag{24d}$$

The left hand side of (24b) can be written as

$$\tau_1 W_1 \log_2\left(1 + \frac{P_a h_1}{W_1 N_0}\right) - \sqrt{W_1}B, \tag{25}$$

where $B = \sqrt{\tau_1}\log_2(e)Q^{-1}(\epsilon_1)$. The first term of (25) is concave and the second term is convex. At the given point W_0, the lower bound of the second term can be given by $-\sqrt{W_1}B \geq -\frac{1}{2}W_{10}^{-\frac{1}{2}}(W_1 - W_{10})$. Using the above lower bound, the problem (24) can be approximated by the following convex problem as

$$\max_{\eta,\mathbf{W}} \ \eta \tag{26a}$$
$$s.t. \ \tau_1 W_1 \log_2\left(1 + \frac{P_a h_1}{W_1 N_0}\right) + C_1^{LB} \geq C_0, \tag{26b}$$
$$\tau_2 W_2 \log_2\left(1 + \frac{P_u h_2}{W_2 N_0}\right) + C_2^{LB} \geq C_0, \tag{26c}$$
$$(16\text{b}), \ (16\text{c}), \ (16\text{d}) \text{ and } (16\text{e}), \tag{26d}$$

where $C_1^{LB} = -\frac{1}{2}W_{10}^{-\frac{1}{2}}(W_1 - W_{10})$ and $C_2^{LB} = -\frac{1}{2}W_{20}^{-\frac{1}{2}}(W_2 - W_{20})$.

It can be seen that problem (26)is convex. In addition, the optimal object value of (26) for that of (23). Therefore, CVX can be used to solve (26) approximately to obtain a sub-optimal the solution of (23).

C. UAV Location Optimization

With fixed duration and bandwidth, the problem (16) can be transformed as

$$\max_{\eta,x} \ \eta \tag{27a}$$
$$s.t. \ (7), \ (8), \ (16\text{b}) \text{ and } (16\text{c}). \tag{27b}$$

With $t = x^2 + H^2$, the left hand side of (5) can be denoted as

$$C_1(t) = \tau_1 W_1\left(\log_2\left(1 + \frac{P_a\beta_0}{W_1 N_0 t}\right) - \sqrt{\frac{V_1}{W_1\tau_1}}\log_2(e)Q^{-1}(\epsilon_1)\right). \tag{28}$$

Following [10], we know that the value of γ_1 is large in the URLLC scenario, and V_1 can be approximated as 1. Then, we can approximate $C_1(t)$ as

$$C_1(t) \approx \tau_1 W_1(\log_2(1 + A_1/t) + A_2) = \tilde{C}_1(t), \tag{29}$$

where $A_1 = \frac{P_a\beta_0}{W_1 N_0}$ and $A_2 = \sqrt{\frac{1}{W_1\tau_1}}\log_2(e)Q^{-1}(\epsilon_1)$. Note that $V_1 \leq 1$, and we have $C_1(t) \geq \tilde{C}_1(t)$.

Since $\tilde{C}_1(t)$ is convex with t, at any given point t_0 its lower bound can be expressed by its first-order Taylor expansion as

$$\tilde{C}_1(t) \geq \tilde{C}_1(t_0) - A_1(t - t_0)/(t^2 + A_1 t) = C_1^{LB}(t). \tag{30}$$

Similarly, denoting the left hand side of (6) as $C_2(s)$, its lower bound can be given as

$$C_2(s) \geq C_2(s_0) - B_1(s - s_0)/(s^2 + B_1 s) = C_2^{LB}(s), \tag{31}$$

where $s = (L-x)^2 + H^2$, $C_2(s) = \tau_2 W_2(\log_2(1 + B_1/s) + B_2)$, $B_1 = \frac{P_u\beta_0}{W_2 N_0}$, and $B_2 = \sqrt{\frac{1}{W_2\tau_2}}\log_2(e)Q^{-1}(\epsilon_2)$.

Similarly, denote the left hand side of (16b) and (16c) as $C_3(s)$ and $C_4(t)$, respectively. At given points s_0 and t_0, their lower bounds can be given by

$$C_3(s) \geq C_3(s_0) - \frac{D_1}{s^2 + D_1 s}(s - s_0) = C_3^{LB}(s), \tag{32}$$

$$C_4(t) \geq C_4(t_0) - \frac{E_1}{t^2 + E_1 t}(t - t_0) = C_4^{LB}(t), \tag{33}$$

where $D_1 = \frac{P_b\beta_0}{W_3 N_0}$ and $E_1 = \frac{P_u\beta_0}{W_4 N_0}$.

Using the above lower bounds, the problem (27) can be approximated by the following convex problem as

$$\max_{\eta,x} \ \eta \tag{34a}$$
$$s.t. \ C_1^{LB}(t) \geq C_0, \tag{34b}$$
$$C_2^{LB}(t) \geq C_0, \tag{34c}$$
$$C_3^{LB}(t) \geq \eta, \tag{34d}$$
$$C_4^{LB}(t) \geq \eta, \tag{34e}$$

which can be approximately solved by CVX.

D. Iterative Algorithm

To solve the problem (16), we propose an iterative algorithm by solving these sub-problems alternately, which is summarized in Algorithm 1. Since the three sub-problems are convex in Algorithm 1, its computational complexity is polynomial.

In Algorithm 1, three convex optimization problems are solved in each iteration with given initial values, and we have

$$\begin{aligned}\eta(\boldsymbol{\tau}^n, \boldsymbol{W}^n, \boldsymbol{x}^n) \leq \eta(\boldsymbol{\tau}^{n+1}, \boldsymbol{W}^r, \boldsymbol{x}^n) \leq \eta(\boldsymbol{\tau}^{n+1}, \boldsymbol{W}^{n+1}, \boldsymbol{x}^n) \\ \leq \eta\left(\boldsymbol{\tau}^{n+1}, \boldsymbol{W}^{n+1}, \boldsymbol{x}^{n+1}\right).\end{aligned} \tag{35}$$

Thus, the objective value of (16) is non-decreasing in each iteration, and the optimal solution to (16) can be considered as its upper bound. Thus, the proposed Algorithm 1 is guaranteed to converge.

Algorithm 1 Iterative Algorithm for Problem (16)

Initialization: Set the feasible initial values $\{\boldsymbol{\tau}^0, \boldsymbol{W}^0, x^0\}$ for the problem (16), and set the maximum number of iterations as N. n denotes the index of iterations.
repeat
  Solve the problem (34) by CVX, and obtain the optimal solution as $\{\boldsymbol{\tau}^n, \boldsymbol{W}^n, x^{n+1}\}$.
  Solve the problem (22) for given $\{\boldsymbol{\tau}^n, \boldsymbol{W}^n, x^{n+1}\}$, and obtain the optimal solution as $\{\boldsymbol{\tau}^{n+1}, \boldsymbol{W}^n, x^{n+1}\}$.
  Solve the problem (24) for given $\{\boldsymbol{\tau}^{n+1}, \boldsymbol{W}^n, x^{n+1}\}$, and denote the optimal solution as $\{\boldsymbol{\tau}^{n+1}, \boldsymbol{W}^{n+1}, x^{n+1}\}$.
  Update: $n = n + 1$.
until $n = N$ or convergence.
Output: $\{\boldsymbol{\tau}, \boldsymbol{W}, x\}$.

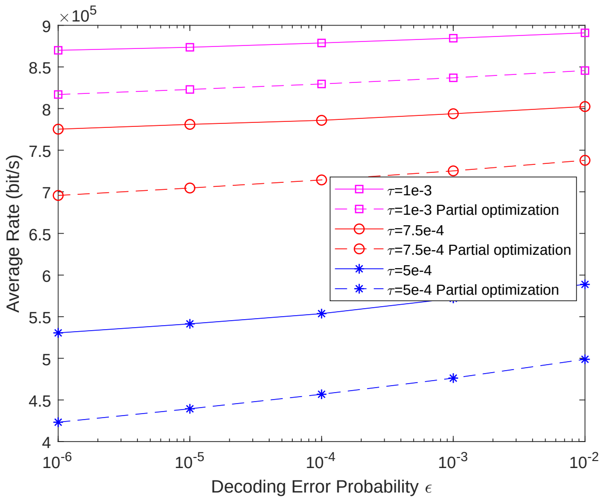

Fig. 3: The average transmission rate of the backward link under different forward link URLLC constraints.

V. Simulation Results and Discussion

The simulation parameters are set as $W = 200$ kHz, $L = 2000$ m, $H = 300$ m, $P_a = 27$ dBm, $P_b = 27$ dBm, $N_0 = -169$ dBm/Hz, the carrier frequency $f = 5$ GHz. Consequently, β_0 can be calculated as $\beta_0 = \left(\frac{c}{4\pi f}\right)^2 \approx 2.2797 \times 10^{-5}$, where c is the light speed.

The average transmission rate of the backward link is shown in Fig. 3, under different duration and decoding error probability constraints, when $P_u = 23$ dBm and $C_0 = 200$ bits. The result with only bandwidth optimization is also provided as a benchmark for comparison, which is denoted as partial optimization. In the partial optimization, the position of the UAV is $x = 1000$ m, and the transmission duration is $\tau_1 = \tau_2 = \tau/2$. From the result, we can see that when the decoding error probability requirement of the forward link decreases, the average transmission rate of the backward link increases. In addition, when the delay constraint in the forward link increases, the backward link average rate also increases. Therefore, the proposed joint optimization algorithm is effective and can outperform the partial optimization scheme. In the simulation, the range of the decoding error probability is from 10^{-6} to 10^{-2}, which contains most of the cases for remote control. In practical systems, the decoding error probability needs to be chosen according to the specific situation.

The average transmission rate of the backward link under different throughput constraints of the forward link is shown in Fig. 4. The partial optimization scheme is also provided for comparison. The decoding error probability constraint is $\epsilon_1 = \epsilon_2 = 10^{-5}$, and the UAV transmit power is $P_u = 23$ dBm. From the result, it can be seen that, the proposed algorithm achieves higher average transmission rate than the partial optimization scheme. With the URLLC throughput requirement of the forward link increasing, the average transmission rate of the backward link decreases. This is because more resource is allocated to the forward link to meet the URLLC requirement. In addition, the decreasing delay of the forward link also leads to the decrease of the average transmission rate of the backward link. In practice, the BS can have fixed power supply and the device is an isolated mobile device. Thus, the BS may have higher transmit power than the device. The case that $P_a = 36$ dBm is shown in Fig. 4(b). The increasing of the BS transmit power leads to a significant increase of the average transmission rate of the backward link.

Fig. 5 plots the average transmission rate of the backward link under different UAV transmit power. From the result we can see that the average transmission rate of the backward link increases when the UAV transmit power increases. Besides, when the forward link can tolerate more delay, higher average transmission rate of the backward link can be achieved. Therefore, the proposed joint optimization algorithm also outperforms the partial optimization scheme in this case.

VI. Conclusions

This correspondence has studied the joint optimization of time, bandwidth and UAV location in a two-way UAV relaying system with the URLLC requirements. The average communication rate of the backward link has been maximized under the URLLC constraint of the forward link. An effective low-complexity iterative algorithm has been proposed to solve the optimization problem alternately for the URLLC-enabled two-way UAV relaying system. Simulation results have shown that significant performance gain can be obtained by the proposed joint resource optimization scheme.

References

[1] X. Pang, M. Sheng, N. Zhao, J. Tang, D. Niyato, and K.-K. Wong, "When UAV meets IRS: Expanding air-ground networks via passive reflection," *IEEE Wireless Commun.*, vol. 28, no. 5, pp. 164–170, Oct. 2021.

[2] N. Zhao, W. Lu, M. Sheng, Y. Chen, J. Tang, F. R. Yu, and K.-K. Wong, "UAV-assisted emergency networks in disasters," *IEEE Wireless Commun.*, vol. 26, no. 1, pp. 45–51, Feb. 2019.

[3] Z. Xiong, Y. Zhang, W. Y. B. Lim, J. Kang, D. Niyato, C. Leung, and C. Miao, "UAV-assisted wireless energy and data transfer with deep reinforcement learning," *IEEE Trans. Cogn. Commun. Netw.*, vol. 7, no. 1, pp. 85–99, Mar. 2021.

[4] X. Jiang, X. Chen, J. Tang, N. Zhao, X. Y. Zhang, D. Niyato, and K.-K. Wong, "Covert communication in UAV-assisted air-ground networks," *IEEE Wireless Commun.*, vol. 28, no. 4, pp. 190–197, Aug. 2021.

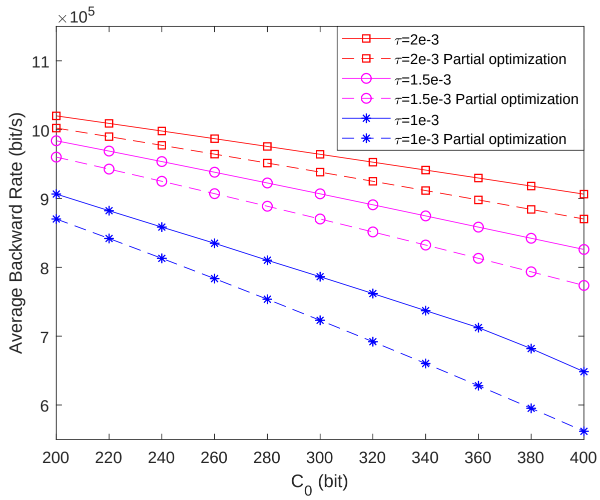

(a) P_a=27dBm

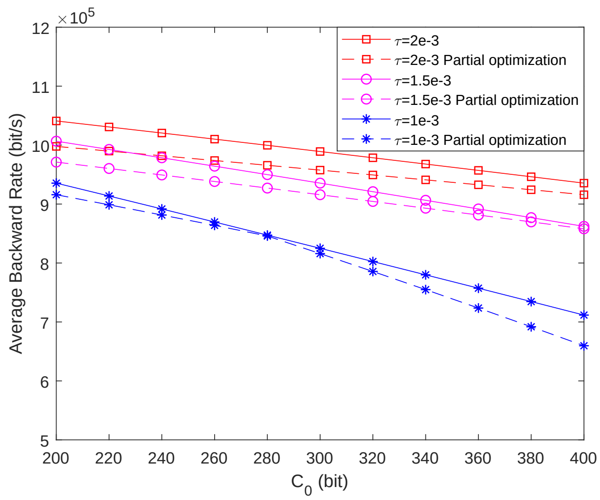

(b) P_a=36dBm

Fig. 4: The average transmission rate of the backward link under different throughput constraints of the forward link.

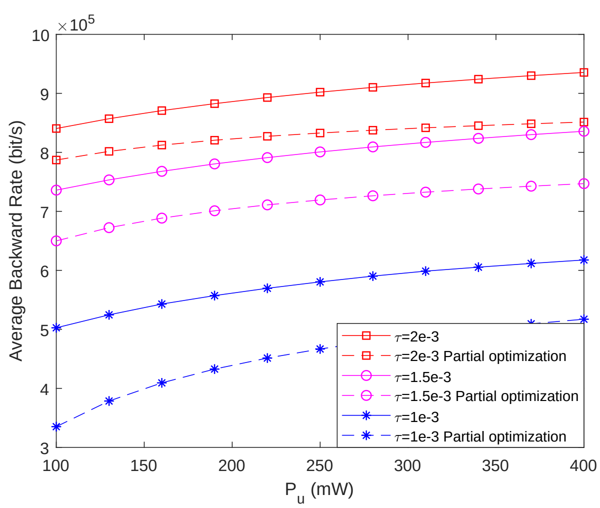

Fig. 5: The average transmission rate of the backward link under different UAV transmit power.

[5] G. Durisi, T. Koch, and P. Popovski, "Toward massive, ultrareliable, and low-latency wireless communication with short packets," *Proc. IEEE*, vol. 104, no. 9, pp. 1711–1726, Aug. 2016.

[6] K. Wang, C. Pan, H. Ren, W. Xu, L. Zhang, and A. Nallanathan, "Packet error probability and effective throughput for ultra-reliable and low-latency UAV communications," *IEEE Trans. Commun.*, vol. 69, no. 1, pp. 73–84, Jan. 2021.

[7] H. Ren, C. Pan, K. Wang, Y. Deng, M. Elkashlan, and A. Nallanathan, "Achievable data rate for URLLC-enabled UAV systems with 3-D channel model," *IEEE Wireless Commun. Lett.*, vol. 8, no. 6, pp. 1587–1590, Dec. 2019.

[8] K. Chen, Y. Wang, Z. Fei, and X. Wang, "Power limited ultra-reliable and low-latency communication in UAV-enabled IoT networks," in *in Proc. IEEE WCNC,* Seoul Korea, pp. 1–6, May 2020.

[9] K. Chen, Y. Wang, J. Zhao, X. Wang, and Z. Fei, "URLLC-oriented joint power control and resource allocation in UAV-assisted networks," *IEEE Internet Things J.*, vol. 8, no. 12, pp. 10103–10116, Jun. 2021.

[10] A. Ranjha and G. Kaddoum, "Quasi-optimization of uplink power for enabling green URLLC in mobile UAV-assisted IoT networks: A perturbation-based approach," *IEEE Internet Things J.*, vol. 8, no. 3, pp. 1674–1686, Feb. 2021.

[11] P. Yang, X. Xi, K. Guo, T. Q. S. Quek, J. Chen, and X. Cao, "Proactive UAV network slicing for URLLC and mobile broadband service multiplexing," *IEEE J. Sel. Areas Commun.*, vol. 39, no. 10, pp. 3225–3244, Oct. 2021.

[12] P. Yang, X. Xi, T. Q. S. Quek, J. Chen, and X. Cao, "Power control for a URLLC-enabled UAV system incorporated with DNN-based channel estimation," *IEEE Wireless Commun. Lett.*, vol. 10, no. 5, pp. 1018–1022, May 2021.

[13] Y. Chen, N. Zhao, Z. Ding, and M.-S. Alouini, "Multiple UAVs as relays: Multi-hop single link versus multiple dual-hop links," *IEEE Trans. Wireless Commun.*, vol. 17, no. 9, pp. 6348–6359, Aug. 2018.

[14] Z. Chang, X. Hou, X. Guo, T. Ristaniemi, and Z. Han, "Secure and energy-efficient resource allocation for wireless power enabled full-/half-duplex multiple-antenna relay systems," *IEEE Trans. Veh. Technol.*, vol. 66, no. 12, pp. 11208–11219, Dec. 2017.

[15] M. Wu, Q. Song, L. Guo, and A. Jamalipour, "Charge-then-cooperate: Secure resource allocation for wireless-powered relay networks with wireless energy transfer," *IEEE Trans. Veh. Technol.*, vol. 70, no. 5, pp. 5088–5093, May 2021.

[16] C. Pan, H. Ren, Y. Deng, M. Elkashlan, and A. Nallanathan, "Joint blocklength and location optimization for URLLC-enabled UAV relay systems," *IEEE Commun. Lett.*, vol. 23, no. 3, pp. 498–501, Mar. 2019.

[17] H. Ren, C. Pan, K. Wang, W. Xu, M. Elkashlan, and A. Nallanathan, "Joint transmit power and placement optimization for URLLC-enabled UAV relay systems," *IEEE Trans. Veh. Technol.*, vol. 69, no. 7, pp. 8003–8007, Jul. 2020.

[18] A. Ranjha and G. Kaddoum, "Quasi-optimization of distance and blocklength in URLLC aided multi-hop UAV relay links," *IEEE Wireless Commun. Lett.*, vol. 9, no. 3, pp. 306–310, Mar. 2020.

[19] X. Xi, X. Cao, P. Yang, J. Chen, T. Q. S. Quek, and D. Wu, "Network resource allocation for eMBB payload and URLLC control information communication multiplexing in a multi-UAV relay network," *IEEE Trans. Commun.*, vol. 69, no. 3, pp. 1802–1817, Mar. 2021.

[20] Y. Polyanskiy, H. V. Poor, and S. Verdu, "Channel coding rate in the finite blocklength regime," *IEEE Trans. Inf. Theory*, vol. 56, no. 5, pp. 2307–2359, 2010.